Available online at www.sciencedirect.com

ScienceDirect

IFAC Papers Online CONFERENCE PAPER ARCHIVE

IFAC-PapersOnLine 49-30 (2016) 325–330

A simplified approach to motion estimation in a UAV using two filters

Gabriel Schmitz * **Tiago Alves** * **Renato Henriques** *
Edison Freitas * **Ebrahim El'Youssef** **

* *UFRGS - Federal University of Rio Grande do Sul, Porto Alegre, RS, Brazil (e-mail: gschmitz@ece.ufrgs.br, talves@ece.ufrgs.br, rventura@ece.ufrgs.br, epfreitas@inf.ufrgs.br).*
** *UFSC - Federal University of Santa Catarina, Florianópolis, SC, Brazil (e-mail: ebrahim.el.youssef@ufsc.br).*

Abstract:
Considering the requirement of precision positioning of Unmanned Aerial Vehicles in applications like in flights formations and flights with collision avoidance, this paper presents the proposal of a composition of a Complementary Filter used in orientation estimation and a Linear Kalman Filter (KF) in position estimation of the UAVs. The data evaluated in the experiments were acquired post flight from the flight controller embedded in a UAV. An Inertial Measurement Unit is used to provide the essentials datasets to the implementation of the Complementary Filter, which is modelled by Euler Angles referenced in a North-East-Down (NED) Coordinate System. The position estimation is obtained using the data from Global Positioning System (GPS) allied to a barometer applied in a Position-Velocity-Acceleration (PVA) model with Linear Kalman Filter. The acquired results provide evidence of the suitability and soundness of the proposed approach.

Keywords: Pose Estimation, Kalman Filter, Sensor Fusion, Complementary Filter, Unmanned Aerial Vehicle.

1. INTRODUCTION

In the last decade 4-Rotor Unmanned Aerial Vehicles (UAVs) have gained popularity due to the simplicity in their construction, ease maintenance, as well as by their flexibility to reach difficult places to access, maneuverability, stability and Vertical Take-Off and Landing capabilities (Abas et al., 2013). They have being used in both civil and military applications such as surveillance, rescue, aerial imagery, structural inspection and maintenance. Due to their suitability and efficiency in accomplishing missions in the mentioned applications, they have received great attention and have been an important research topic (Teulière et al., 2010; Zhang et al., 2015).

One of the trend topics in the development of UAVs is related to state estimation. It covers both states of motion and posture information such as velocity, acceleration, heading, tilt and rotation angles. Also reliable motion control and pose estimation are basic requirements to achieve autonomous flight (Hong et al., 2014; Xu Wanli et al., 2014). The most common setting used to ensure a reasonable state estimation is the sensorial fusion. It could be seen as a process that utilizes data from one or more sensors to reduce the uncertainty of the others sensors measures. Filtering techniques are also used to improve the accuracy of the data acquired from sensors. An example of sensorial fusion is based on the Extended Kalman Filter (Gelb, 1974) applied to optimally fuse gyroscopes and accelerometer measurements (Abeywardena and Munasinghe, 2010).

The advances in aerial robotics research allowed multiple UAVs be cooperatively used to carry out tasks that can not be easily done by a single robot (Alejo et al., 2009). They use strategies known as tactics, which are defined as the procedure used by the UAV team to execute a mission and that can be either centralized, in which a decision maker sends coordinated instructions to a group of UAVs or decentralized, in which each of them is responsible for making its individual decisions. There are consistent tactics which can be classified as swarming or formation, task assignment, formation reconfiguration and dynamic encirclement and both of them require accurate pose estimation and collision avoidance methods to accomplish their tasks. (Hafez et al., 2015).

This work presents a position estimation strategy based in a random motion, considered as a Position-Velocity-Acceleration (PVA) model, using a Linear Kalman Filter together with the measurements of Global Positioning System (GPS) and Barometer to approximate the true movement. An approach to orientation estimation, based on a complementary filter performing sensorial fusion, will also be demonstrated.

This paper is structured as follows: Section 2 presents a literature review. In Section 3, the mathematical modelling and fundamentals of the proposed solution are demonstrated. The numerical results are presented and discussed in Section 4. Section 5 presents the conclusions and the directions for future works.

2405-8963
Peer review under responsibility of International Federation of Automatic Control.
10.1016/j.ifacol.2016.11.156

2. RELATED WORKS

The pose estimation was treated in (Filipe et al., 2015) applying a Dual Quaternion Multiplicative Extended Kalman Filter (DQ-MEKF). This technique is an extension of the Quaternion Multiplicative Extended Kalman Filter (Lefferts et al., 1982) widely employed for spacecraft attitude estimation, using the dual quaternion multiplication and the concept of error unit dual quaternion.

In (Blachuta et al., 2014), the relationship between the measured signals, on each axis in the sensor coordinates, and the inertial coordinates were defined by the Euler angles, respectively by roll (ϕ), pitch (θ) and yaw (ψ) angles, as a specific sequence of rotation with respect to x, y and z axes of a referred coordinate system. The axes of inertial coordinate system were defined as a right handed Cartesian coordinate system with North, West and Upward (NWU) directions.

In (Huang et al., 2015), the Euler angles were utilized to find the transformation matrix which relates the North-East-Down (NED) frame and the body frame. Furthermore, the Euler angles were determined from the gyroscope, magnetometer and accelerometer to implement the Complementary Filter.

In (Challa et al., 2016), a quaternion-based attitude unscented Kalman filter was formulated with quaternion errors parametrized by small angle approximations considering a magnetometer-only spacecraft scenario. The method was applied to a filter with a state vector consisting of the attitude quaternion and the gyro bias vector.

A generalized complementary filter (GCF) was proposed by (LI, Xiang et al., 2015) for attitude estimation. The GCF was based on the vector observation and its cross product. The results from the GCF had better numerical stability and much higher computational efficiency than the multiplicative extended Kalman filter (MEKF).

3. METHODOLOGY

3.1 Position Estimation

The linear motion in each of the axis (x, y, z) was defined as a unidimensional random motion. The random motion was considered as a Position-Velocity-Acceleration (PVA) model. As could be seen in Fig. 1, the acceleration is modeled as the integral of the white noise (Brown and Hwang, 2012).

Since the model is based in a random walk process, it does not reflect the real movement of the UAV. The embedded sensors are therefore used to approximate the real motion based on PVA model.

In the considered PVA model where the input is a Gaussian noise, all states are non-stationary. Due to this fact and also according to (Brown and Hwang, 2012), this model is only useful in the cases where measurements can be used to bound the states.

A linear Kalman Filter (Kalman, 1960) was chosen to handle with the motion model. The process to be estimated in the filter was defined in the equation (1), where $\boldsymbol{\Phi}_k$ is the state transition matrix, $\boldsymbol{H}_k$ is the state observation matrix and $\boldsymbol{w}_k$ an $\boldsymbol{v}_k$ are both uncorrelated Gaussian white noise.

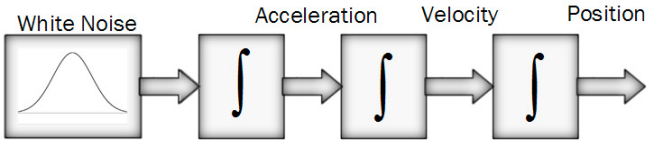

Fig. 1. Position-Velocity-Acceleration (PVA) Model (Brown and Hwang, 2012).

$$\begin{aligned} \boldsymbol{x}_{k+1} &= \boldsymbol{\Phi}_k \boldsymbol{x}_k + \boldsymbol{w}_k \\ \boldsymbol{z}_k &= \boldsymbol{H}_k \boldsymbol{x}_k + \boldsymbol{v}_k \end{aligned} \tag{1}$$

The linear motion state-vector (2) has nine states, where P defines position, V velocity and A acceleration for each axis. Following the basic concepts of kinematics and also to be consistent with equation (2), the state transition matrix $\boldsymbol{\Phi}_k$ (4) is derived for a particular unidimensional case from equation (3) and thus extended to three-dimensional case (Gibbs, 2011).

$$\boldsymbol{x}_k = \begin{bmatrix} Px_k & Py_k & Pz_k & Vx_k & Vy_k & Vz_k & Ax_k & Ay_k & Az_k \end{bmatrix}^T \tag{2}$$

$$\begin{bmatrix} \dot{P} \\ \dot{V} \\ \dot{A} \end{bmatrix} = \overbrace{\begin{bmatrix} 0 & 1 & 0 \\ 0 & 0 & 1 \\ 0 & 0 & 0 \end{bmatrix}}^{\mathbf{F}} \begin{bmatrix} P \\ V \\ A \end{bmatrix} + \begin{bmatrix} 0 \\ 0 \\ Q \end{bmatrix}$$

$$\boldsymbol{\Phi} = \mathbf{I} + \mathbf{F}\Delta t + \frac{(\mathbf{F}\Delta t)^2}{2} = \begin{bmatrix} 1 & \Delta t & \frac{1}{2}\Delta t^2 \\ 0 & 1 & \Delta t \\ 0 & 0 & 1 \end{bmatrix} \tag{3}$$

The measurements utilized to bound the PVA model are acquired from a Global Positioning System (GPS) and also from a barometer sensor. The first of them is used to acquire latitude and longitude data and the other to acquire altitude data. The measurement vector $\boldsymbol{z}_k$ is defined as in the equation (5) where Px_{g_k} defines the latitude, in degrees, Py_{g_k} the longitude, in degrees, and Pz_{b_k} the altitude, in meters (AG, 2013).

$$\boldsymbol{\Phi}_k = \begin{bmatrix} \mathbf{I}_{3x3} & \Delta t * \mathbf{I}_{3x3} & \frac{1}{2}\Delta t^2 * \mathbf{I}_{3x3} \\ \mathbf{0}_{3x3} & \mathbf{I}_{3x3} & \Delta t * \mathbf{I}_{3x3} \\ \mathbf{0}_{3x3} & \mathbf{0}_{3x3} & \mathbf{I}_{3x3} \end{bmatrix}_{9x9} \tag{4}$$

$$\boldsymbol{z}_k = \begin{bmatrix} Px_{g_k} & Py_{g_k} & Pz_{b_k} \end{bmatrix} \tag{5}$$

North-East-Down (NED) Coordinate System The NED coordinate system is a coordinate frame fixed to the earth's surface. It is also known as ground or navigation coordinate system. In the Fig. 2 are defined the origin and axes from this coordinate system (Cai et al., 2011).

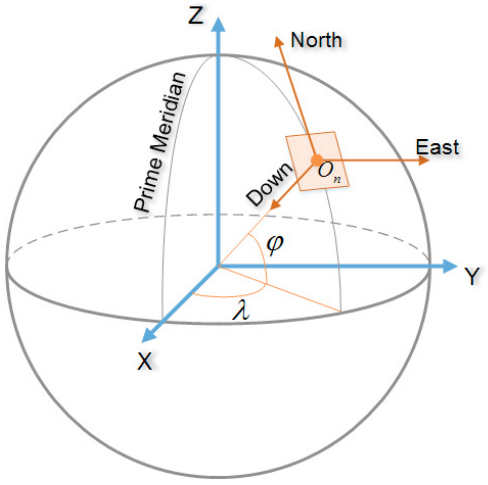

Fig. 2. NED Coordinate System. (Huang et al., 2015).

1. The origin (denoted by O_n) is arbitrarily fixed to a point on the earth's surface.

2. The X-axis (denoted by North) points toward the geodetic north.

3. The Y-axis (denoted by East) points toward the geodetic east.

4. The Z-axis (denoted by Down) points downward along the ellipsoid normal.

In flight control and navigation, the NED frame fulfills a very important role, the navigation of small-scale is normally carried out within this frame (Cai et al., 2011). The flight control used in the UAVs of this project utilizes the NED coordinate system to the UAV positioning.

The Linear Kalman Filter A Kalman filter is an optimal recursive data processing algorithm (Maybeck, 1979). It was proposed in 1960 to deal with optimal estimation in discrete systems and has the advantage of handle the system in a state-space setting. Because of its recursive characteristic, it does not require all previous data to evaluate every new measurement (Brown and Hwang, 2012; Maybeck, 1979).

Suppose a system model like $\boldsymbol{x}_{k+1} = \boldsymbol{\Phi}_k \boldsymbol{x}_k + \boldsymbol{w}_k$ and a measurement model like $\boldsymbol{z}_k = \boldsymbol{H}_k \boldsymbol{x}_k + \boldsymbol{v}_k$ which reflects the equation (1). The equations (12), (13) and (14) define the covariance matrices for the uncorrelated noises $\boldsymbol{w}_k$ and $\boldsymbol{v}_k$ (Brown and Hwang, 2012).

The filter process could be seen as two steps, the first one prediction and the last one update. The prediction step is defined by the equations (6) and (7) and utilizes a previous estimate to obtain an atual estimation. The update step is defined by the equations (8), (9) and (10) and fuses the estimation in the prediction step with the atual observation to improve the state estimated (Brown and Hwang, 2012).

$$\hat{\boldsymbol{x}}_{k+1}^{-} = \boldsymbol{\Phi}_k \hat{\boldsymbol{x}}_k \quad (6)$$

$$\boldsymbol{P}_{k+1}^{-} = \boldsymbol{\Phi}_k \boldsymbol{P}_k \boldsymbol{\Phi}_k^T + \boldsymbol{Q}_k \quad (7)$$

$$\boldsymbol{K}_k = \boldsymbol{P}_k^{-} \boldsymbol{H}_k^T (\boldsymbol{H}_k \boldsymbol{P}_k^{-} \boldsymbol{H}_k^T + \boldsymbol{R}_k)^{-1} \quad (8)$$

$$\hat{\boldsymbol{x}}_k = \hat{\boldsymbol{x}}_k^{-} + \boldsymbol{K}_k (\boldsymbol{z}_k - \boldsymbol{H}_k \hat{\boldsymbol{x}}_k^{-}) \quad (9)$$

$$\boldsymbol{P}_k = (\boldsymbol{I} - \boldsymbol{K}_k \boldsymbol{H}_k) \boldsymbol{P}_k^{-} \quad (10)$$

$$\boldsymbol{P}_k = (\boldsymbol{I} - \boldsymbol{K}_k \boldsymbol{H}_k) \boldsymbol{P}_k^{-} (\boldsymbol{I} - \boldsymbol{K}_k \boldsymbol{H}_k)^T + \boldsymbol{K}_k \boldsymbol{R}_k \boldsymbol{K}_k^T \quad (11)$$

$$E[\boldsymbol{w}_k \boldsymbol{w}_i^T] = \begin{cases} \boldsymbol{Q}_k, & i = k \\ \boldsymbol{0}, & i \neq k \end{cases} \quad (12)$$

$$E[\boldsymbol{v}_k \boldsymbol{v}_i^T] = \begin{cases} \boldsymbol{R}_k, & i = k \\ \boldsymbol{0}, & i \neq k \end{cases} \quad (13)$$

$$E[\boldsymbol{w}_k \boldsymbol{v}_i^T] = 0, \forall k, i \quad (14)$$

The equation (10) determines the error covariance and is only valid for the optimal gain condition. For the suboptimal or even the optimal case, the equation (11) is most appropriate. The propagation of the state estimation and of the error covariance are performed by equations (6) and (7), the Kalman gain is calculated by (8) and the update of the state estimation is performed by (9) (Brown and Hwang, 2012; Maybeck, 1979).

3.2 Orientation Estimation

The X, Y and Z axes of the inertial coordinate system were defined as North, East and Downward directions demonstrated in the Fig. 2. The directions of the rotated entity, usually called the body coordinate, are defined by the Euler angles, which defines the attitudes of an entity by yaw(ψ), pitch(θ) and roll(ϕ) angles (Tseng and Chen, 2011).

The transformation between the inertial and body coordinates can then be defined by the equation (16), through the direction cosine matrix considering the $R_3(\phi) R_2(\theta) R_1(\psi)$ rotations and x_b, y_b and z_b like the body coordinate vector, shown by the equation (15).

$$\left[C_b^n\right] = \begin{bmatrix} C_\psi C_\theta & -S_\psi C_\theta + C_\psi S_\theta S_\phi & S_\psi S_\phi + C_\psi S_\theta C_\phi \\ S_\psi C_\theta & C_\psi C_\phi + S_\psi S_\theta S_\phi & -C_\psi S_\phi + S_\psi S_\theta C_\phi \\ -S_\theta & C_\theta S_\phi & C_\theta C_\phi \end{bmatrix} \quad (15)$$

$$\begin{bmatrix} X & Y & Z \end{bmatrix}^T = \left[C_b^n\right] \begin{bmatrix} x_b & y_b & z_b \end{bmatrix}^T \quad (16)$$

In equation (15), C_i is cos(i) and S_i is sin(i) and they can be defined as vectors in the Downward and North directions (Tseng and Chen, 2011).

The gyroscopes measure angular rates $\boldsymbol{\omega} = \begin{bmatrix} \omega_x & \omega_y & \omega_z \end{bmatrix}^T$ with respect to body reference frame. However this type of sensor suffer the effects of noise and drift and thus the simple integration of angular rates is not enough to get the attitude. The relations between angular rates in the body frame and the time derivatives of the Euler angles in

the inertial frame are represented by (17-18) (Fux, 2008; Tseng and Chen, 2011).

$$\begin{bmatrix}\omega_x\\ \omega_y\\ \omega_z\end{bmatrix} = \begin{bmatrix}1 & 0 & -\sin(\theta)\\ 0 & \cos(\phi) & \cos(\theta)\sin(\phi)\\ 0 & -\sin(\phi) & \cos(\theta)\cos(\phi)\end{bmatrix}\begin{bmatrix}\dot{\phi}\\ \dot{\theta}\\ \dot{\psi}\end{bmatrix} \quad (17)$$

$$\begin{bmatrix}\dot{\phi}\\ \dot{\theta}\\ \dot{\psi}\end{bmatrix} = \begin{bmatrix}1 & \sin(\phi)\tan(\theta) & \cos(\phi)\tan(\theta)\\ 0 & \cos(\phi) & -\sin(\phi)\\ 0 & \frac{\sin(\phi)}{\cos(\theta)} & \frac{\cos(\phi)}{\cos(\theta)}\end{bmatrix}\begin{bmatrix}\omega_x\\ \omega_y\\ \omega_z\end{bmatrix} \quad (18)$$

The attitude relations (ϕ, θ) can be estimated through the utilization of the projected vectors of gravity measured by accelerometers and (ψ) through the measurement of the earth magnetic field acquired from magnetometers. Accelerometers measure the linear acceleration of the body and when this linear acceleration is smaller than gravitational acceleration, this sensor provides the components of the gravity in the body frame (Fux, 2008).

The magnetometers measure local magnetic field vector in the the body reference frame. Both accelerometer and magnetometer suffer with bias and noise. The magnetometer, however, suffer also with distortion in the measurement due to ferromagnetic elements in its vicinity and also due to electromagnetic fields irradiated over the sensor. The equations (19-21) provide the relations between normalized accelerometer measurements (22), normalized magnetometer measurements (23-24) and the Euler angles. In this formulation, when the pitch (20) reaches $\pm 90°$, the roll (19) should be set to $0°$ to avoid singularities and also when ($M_{yn} < 0$), yaw (21) need to be added to $360°$(Fux, 2008; ST-Microelectronics, 2010; Tseng and Chen, 2011).

$$\phi = \sin^{-1}\left(\frac{A_{yn}}{\cos(\theta)}\right) \quad (19)$$

$$\theta = \sin^{-1}(-A_{xn}) \quad (20)$$

$$\psi = \tan^{-1}\left(\frac{M_{yn}}{M_{xn}}\right) \quad (21)$$

$$A_{xn} = \frac{A_x}{\|A\|},\ A_{yn} = \frac{A_y}{\|A\|},\ A_{zn} = \frac{A_z}{\|A\|} \quad (22)$$

$$M_{xn} = \frac{M_x}{\|M\|}\cos(\theta) + \frac{M_z}{\|M\|}\sin(\theta), \quad (23)$$

$$M_{yn} = \frac{M_x}{\|M\|}\sin(\phi)\sin(\theta) + \frac{M_y}{\|M\|}\cos(\phi) - \frac{M_z}{\|M\|}\sin(\phi)\cos(\theta) \quad (24)$$

3.3 Complementary Filter

Although the body's orientation estimation can be found through the equations (19-21), sensors like Gyroscope, Accelerometer and Magnetometer cannot provide enough accuracy to allow directly use of these relations (Gui et al., 2015; Tseng and Chen, 2011). To cope with the MEMS sensors characteristics, which can complement each other to achieve more accurate measurement, Colton (2007) demonstrated a simpler approach than the traditional complex filters, named The Complementary Filter.

The behaviour of this filter is described according with Fig. (3) and its mathematical model is determined by equation (25). The variable φ defines the angle (Roll, Pitch or Yaw), α is the filter coefficient, $\boldsymbol{\omega_{gyr}}$ is the gyroscope angular-rate (ω_{gyrx}, ω_{gyry} or ω_{gyrz}) and $\varphi_{Aacc/Mag}$ is the Angle (Roll, Pitch or Yaw) found with the accelerometer or also by magnetometer. The coefficient α is obtained from (26) where τ is the time constant of the filter (Gui et al., 2015).

$$\varphi_k = \alpha * (\varphi_{k-1} + \omega_{Gyr(k)} * \Delta t) + (1-\alpha) * \varphi_{Acc(k)} \quad (25)$$

$$\alpha = \frac{\tau}{\tau + \Delta t} \quad (26)$$

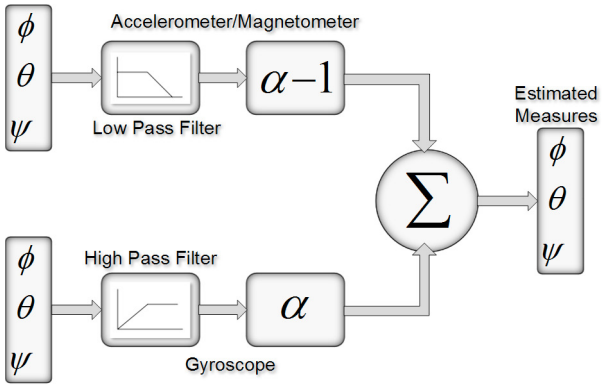

Fig. 3. Complementary Filter (Colton, 2007)

4. RESULTS

The evaluation of a pos-flight dataset, recorded in may of 2016, was performed. This dataset covered approximately 16 minutes of flight with an 3DR Iris+ UAV over one of the campi of the Federal University of Rio Grande do Sul, located in Porto Alegre-Brazil.

The UAV has a PixHawk PX4 Autopilot, flight controller unit, responsible for receiving commands, control the trajectory and also to register all the received commands and sensor data along the flight.

From this dataset it was used the RAW data of gyroscope, accelerometer, barometer, magnetometer and GPS. The evaluation was performed without the calibration parameters of the sensors because the dataset utilized was provided with an offline information.

The data from GPS and barometer were utilized to estimate the linear motion of the UAV. A Kalman filter was used with a PVA model to handle with the low sample rate of the GPS. The results are shown in table (1) and figures (4) - (6) present the GPS sampled data and the estimated data.

The data from accelerometer, magnetometer and gyroscope were utilized to estimate the orientation of the

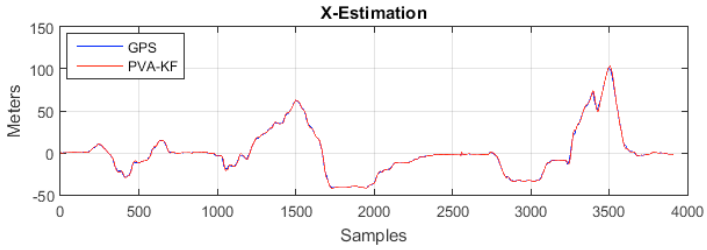

Fig. 4. Position Estimation - X-Axis

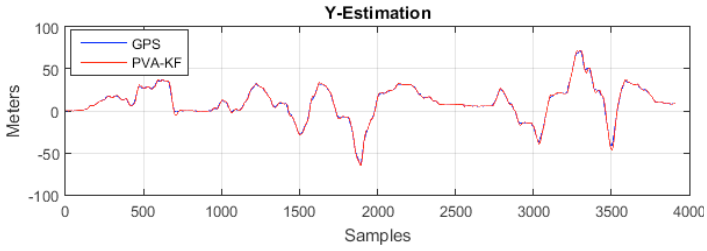

Fig. 5. Position Estimation - Y-Axis

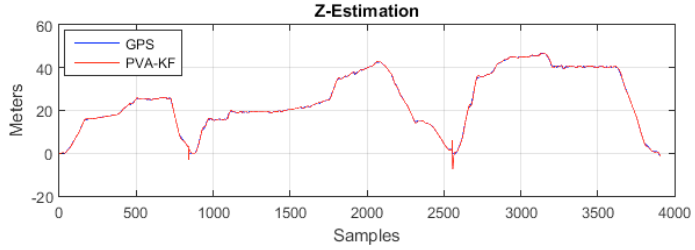

Fig. 6. Position Estimation - Z-Axis

UAV. A complementary filter, which is simpler than the Extended Kalman Filter, was utilized to fuse data from the sensors and as could be seen in figures (7)-(9), the Roll and Pitch estimates are near to PixHawk EKF estimation. The Yaw angle does not show the same behaviour as the two previous estimates, the results are shown in table (1). The magnetometer measurements are more sensitive to external factors as proximity to metals and irradiated electromagnetic fields. Besides that, a calibration of the sensor to eliminate misalignment was not performed. However this estimate tends to approximate the same shape as the Pixhawk estimation with a continuous offset of approximately 6 degrees.

One of the challenges in evaluating the results and in comparing them to those presented by the PixHawk is related to number of samples. Each sensor has a sample rate and therefore the measurements have different number of samples. The magnetometer measures, due to sensor rate, do not have the same number of samples that gyroscope and accelerometer reaches. The magnetometer data were replicated to allow the Yaw evaluation together with the other two previous sensors, collaborating to reduce the precision in the sensor fusion. In the rating with the PixHawk data, the estimation had to be resampled to match the same number of the others sensors.

The filter parametrization was done empirically based in analyse of the results in simulation comparing to a commercial flight control hardware.

Table 1. Error Evaluation

	Min	Mean	Max	Unit
P_x	0	0.5756	5.9690	(m)
P_y	0	0.7572	6.8498	(m)
P_z	0	0.1777	8.0311	(m)
$Roll\ (\phi)$	0.0021	0.9986	7.9052	$(^\circ)$
$Pitch\ (\theta)$	0.0049	1.2058	7.2918	$(^\circ)$
$Yaw\ (\psi)$	4.5023	6.1805	7.1903	$(^\circ)$

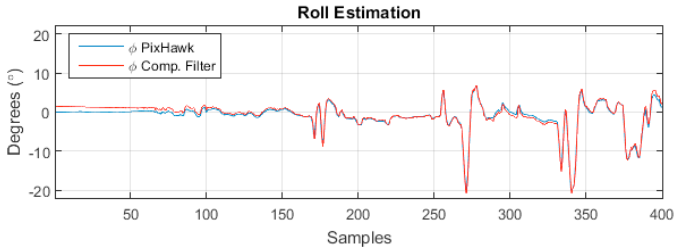

Fig. 7. Roll Estimation

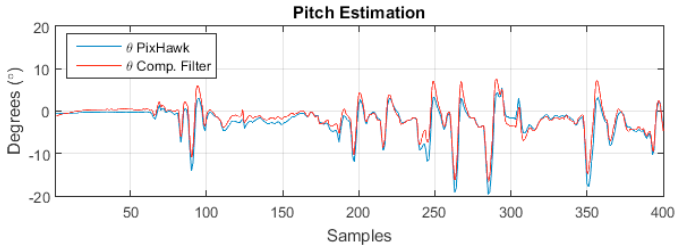

Fig. 8. Pitch Estimation

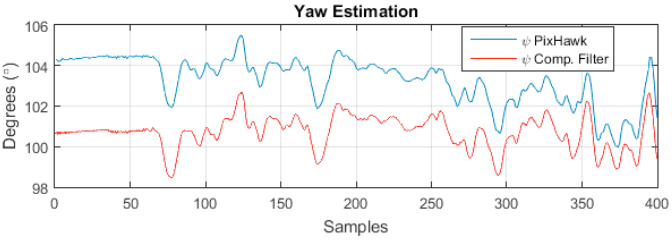

Fig. 9. Yaw Estimation

5. CONCLUSIONS AND FUTURE WORKS

In this paper two filters were presented to parameters estimation, firstly was shown a Kalman filter based in a PVA model to estimate the position of the UAV and after a Complementary Filter, which was used to achieve the orientation of this UAV.

The first of them follows a random-walk model which is bounded by the utilized sensors and the Kalman filter. The results achieved are able to be used in future applications where precision is required. The other one, although simple, presented acceptable results to be embedded in a low complexity flight controller since the errors could easily be reduced by the software and with the proper sensory calibration. It is noteworthy the complementary filter is simpler than the EKF mainly due to scalar nature of its math operations. The complexity of the EKF is related to its matrix operations, but it is important to highlight the EKF algorithm in general is more robust.

The future directions consist in a development of a unique Extended Kalman Filter to improve the sensory fusion

using all the sensors provided in PixHawk PX4 or another flight controller platform. Finally, a high-level complementary filter is intended to be evaluated aiming the accuracy improvement in orientation estimation.

REFERENCES

Abas, N., Legowo, A., Ibrahim, Z., Rahim, N., and Kassim, A.M. (2013). Modeling and System Identification using Extended Kalman Filter for a Quadrotor System. *Appl. Mech. Mater.*, 313-314, 976–981. doi: 10.4028/www.scientific.net/AMM.313-314.976.

Abeywardena, D.M.W. and Munasinghe, S.R. (2010). Performance analysis of a Kalman Filter based attitude estimator for a Quad Rotor UAV. In *International Congress on Ultra Modern Telecommunications and Control Systems*, 466–471. IEEE. doi: 10.1109/ICUMT.2010.5676596.

AG, U.b. (2013). u-blox 6 - Receiver Description. 210.

Alejo, D., Conde, R., Cabana, J.A., and Ollero, A. (2009). Multi-UAV collision avoidance with separation assurance under uncertainties. *IEEE 2009 International Conference on Mechatronics, ICM 2009*, 00(April), 1–6. doi: 10.1109/ICMECH.2009.4957235.

Blachuta, M., Grygiel, R., Czyba, R., and Szafranski, G. (2014). Attitude and heading reference system based on 3D complementary filter. *2014 19th International Conference on Methods and Models in Automation and Robotics, MMAR 2014*, 851–856.

Brown, R. and Hwang, P. (2012). *Introduction to Random Signals and Applied Kalman Filtering with Matlab Exercises*. CourseSmart Series. Wiley.

Cai, G., Chen, B.M., and Lee, T.H. (2011). Coordinate Systems and Transformations. 23–34. doi:10.1007/978-0-85729-635-12.

Challa, M.S., Moore, J.A.Y.G., and Rogers, D.J. (2016). A Simple Attitude Unscented Kalman Filter: Theory and Evaluation in a Magnetometer-Only Spacecraft Scenario. 1845–1858.

Colton, S. (2007). The Balance Filter. Technical report, Massachusetts Institute of Technology, Cambridge.

Filipe, N., Kontitsis, M., and Tsiotras, P. (2015). Extended Kalman Filter for Spacecraft Pose Estimation Using Dual Quaternions. *Journal of Guidance, Control, and Dynamics*, 38(9), 1–17. doi:10.2514/1.G000977.

Fux, S. (2008). *Development of a planar low cost Inertial Measurement Unit for UAVs and MAVs*. Msc dissertation, Swiss federal Institute of Technology Zurich.

Gelb, A. (1974). *Applied Optimal Estimation*. MIT Press, 1 edition.

Gibbs, B.P. (2011). *Advanced Kalman Filtering, Least-Squares and Modeling: A Practical Handbook*. Wiley.

Gui, P., Tang, L., and Mukhopadhyay, S. (2015). MEMS based IMU for tilting measurement: Comparison of complementary and kalman filter based data fusion. *2015 IEEE 10th Conf. Ind. Electron. Appl.*, 2004–2009. doi:10.1109/ICIEA.2015.7334442.

Hafez, A.T., Givigi, S.N., Ghamry, K.A., and Yousefi, S. (2015). Multiple cooperative UAVs target tracking using Learning Based Model Predictive Control. In *2015 International Conference on Unmanned Aircraft Systems (ICUAS)*, 1017–1024. IEEE. doi: 10.1109/ICUAS.2015.7152391.

Hong, Y., Lin, X., and Zhuang, Y. (2014). Real-Time Pose Estimation and Motion Control for a Quadrotor UAV. *Proceeding 11th World Congr. Intell. Control Autom. Shenyang, China*, 2370–2375.

Huang, Y.h., Rizal, Y., and Ho, M.t. (2015). Development of Attitude and Heading Reference Systems. 13–18.

Kalman, R.E. (1960). A new approach to linear filtering and prediction problems. *Journal of basic Engineering*, 82(1), 35–45.

Lefferts, E.J., Markley, F.L., and Shuster, M.D. (1982). Kalman Filtering for Spacecraft Attitude Estimation. *AIAA 20th Aerospace Sciences Meeting*, 5(5), 417–429. doi:10.2514/3.56190.

LI, Xiang, HE, Chuan, WANG, Yongjun, and LI, Zhi (2015). Generalized complementary filter for attitude estimation based on vector observations and cross products *. (August), 1733–1737.

Maybeck, P. (1979). *Stochastic Models, Estimation and Control*. Number pt. 1 in Mathematics in science and engineering. Academic Press.

ST-Microelectronics (2010). Application note Using LSM303DLH for a tilt compensated electronic compass. *Using LSM303DLH a tilt Compens. Electron. compass*, AN3192(August 2010), 1–34.

Teulière, C., Eck, L., Marchand, E., and Guénard, N. (2010). 3D model-based tracking for UAV position control. *IEEE/RSJ 2010 Int. Conf. Intell. Robot. Syst. IROS 2010 - Conf. Proc.*, 1084–1089. doi: 10.1109/IROS.2010.5649700.

Tseng, S.P. and Chen, C.s. (2011). Motion and Attitude Estimation Using Inertial Measurements with Complementary Filter. *Asian Control Conference*, 863–868.

Xu Wanli, Bao Shuo, and Liu Zhun (2014). The state estimation of UAV based on UKF. *2014 IEEE Workshop on Advanced Research and Technology in Industry Applications (WARTIA)*, (3), 402–405. doi: 10.1109/WARTIA.2014.6976280.

Zhang, Y., Zhang, Y., Mu, X., and Wang, Y. (2015). Pose Control of Quadrotor Unmanned Aerial Vehicle Based on Double Filters. (61471110), 298–304.